Received: 17 April 2022 | Accepted: 1 June 2022
DOI: 10.1049/elp2.12222

IET Electric Power Applications
The Institution of Engineering and Technology WILEY

ORIGINAL RESEARCH

Model-based online efficiency control of induction motor drives based on nonlinear technique

Hamidreza Mosaddegh Hesar | **Mojtaba Ayaz Khoshhava** | **Hossein Abootorabi Zarchi**

Department of Electrical Engineering, Ferdowsi University of Mashhad, Mashhad, Iran

Correspondence
Hossein Abootorabi Zarchi, Department of Electrical Engineering, Ferdowsi University of Mashhad, Mashhad 91775-1111, Iran.
Email: abootorabi@um.ac.ir

Funding information
Research Deputy of Ferdowsi University of Mashhad, Grant/Award Number: 50239

[Correction added on 20 June 2022, after first online publication: Changes made in the funding statement and acknowledgment sections.]

Abstract
To accomplish benefits such as high accuracy and fast response, the model-based loss minimisation algorithms (LMAs) are introduced in the literature, as one of the main available techniques for minimising power losses in electrical motors. They are appropriate for dynamic applications, which necessitate very fast update of the control variable. This study proposes a novel real-time LMA based on super-twisting sliding mode controller (SMC) for induction motor (IM) drives, while keeping a good dynamic response. In this regard, a loss minimisation criterion for the efficiency optimisation is proposed and scrutinised. It is shown analytically that LMA will be realised if the nonlinear controller forces this criterion to zero. Moreover, a super-twisting SMC integrated with the iron loss is proposed which directly regulates both the power loss-minimising criterion and the electromagnetic torque by choosing those as control outputs. The stability of the super-twisting SMC is also verified through the Lyapunov's stability principle. The complete closed-loop control of the proposed LMA-based IM drive is successfully implemented in real-time using a digital signal processor board TMS320F28335 for a laboratory 3-phase IM drive of 2.2 kW. The performance and functionality of the proposed scheme are assessed through experimental results.

1 | INTRODUCTION

Induction motors are broadly used in industry applications, thanks to their rugged construction, low maintenance cost and high reliability. In this regard, energy saving is an essential issue and this is why noticeable attempts have been accomplished to increase their efficiency. The loss minimisation is carried out either in the manufacturing process by finite element design and construction approaches [1, 2], or by using loss minimisation approaches (LMAs). The principle objective of the latter field is to adjust the magnitude of motor flux according to the given operating points.

Generally, there exist two methods in order to optimise the efficiency in ac motor drives. One of them is based on the model and the other is based on the search. In model-based methods, loss-minimisation strategy is implemented in the motor loss model [3–10]. In this regard, the loss minimisation criterion is found by differentiating the expression of electrical power losses with respect to variables such as the d-axis component of stator current [3], slip speed [4], and flux [6]. The other approach is independent of load conditions and motor parameters and can be applied to any type of control system and electrical motor [11–13]. In this method, for desired rotor speed and load torque, a control variable such as reference flux is slowly adjusted to minimise the input power. To remove the instability of the motor drive system, the reference flux should change accordingly if an unexpected event occurs in the load. Besides these two methods, hybrid ones have been introduced in recent years [14, 15]. The hybrid methods are more sensitive to variation of parameters compared to search-based approaches and are also slower than model-based algorithms.

In ref. [3], first, the optimal magnitude of the magnetising current is determined in the Rotor flux oriented (RFO) reference frame. To obtain the optimal current for loss minimisation, electrical losses are then derived in terms of stator current. Nevertheless, variations of iron loss resistance are not considered in different operating conditions. In ref. [5], even though the iron loss is neglected, the proposed LMA has taken into account the saturation effect which can be utilised in both transient and in steady-state conditions. A loss model has been proposed for linear IM drive in [6], including both inverter and motor losses. According to this model, a model-based loss minimisation algorithm has been developed in the steady-state condition. For an IM and inverter set, an efficiency optimisation algorithm has been introduced based on the concept of system-level loss minimisation by *Sridharan et al.* [8]. System-level techniques commonly minimise overall losses including losses in the machine, inverter, dc-link, and filter. Compared to component-based techniques such as minimising motor losses, these strategies are more comprehensive. In ref [9], the ratio of d-axis to q-axis of the magnetising current is regulated to minimise the electrical losses. In ref [12], efficiency of the sliding mode-based IM drive is optimised for each mechanical load and rotor speed by adjusting the magnitude of the stator flux. In this control scheme, the input power is chosen as an objective function rather than stator current. To reduce the convergence time, the reference flux is changed in large steps at the beginning of the search process and then small flux reduction steps are selected to maintain stability.

This study introduces a model-based loss minimisation scheme in combination with the super-twisting sliding mode controller (SMC) controller for three-phase IM drives. In this regard, the errors of electromagnetic torque and LMA criterion with respect to reference values are delivered to the proposed controller.

Control of IM constitutes a theoretically challenging problem, due to the presence of nonlinear dynamics. The implementation of SMC for IM in ref. [16], demonstrates the robustness of this control approach to variations of IM parameters. The benefits of SMC are high robustness, disturbance cancelation, simple implementation, and fast responses during transients. The stabilisation time of this controller is not, however finite, and controlled states of the system are affected by chattering phenomena. To remove the SMC disadvantages, the integral-SMC has been introduced for IM by Barambones *et. al* [17], in which the global asymptotic speed tracking is provided considering parameter uncertainties and load torque. The prerequisite of this control approach is, however, a discrete control action with high switching frequency. The second-order SMC is an alternative solution which relieves chattering in the presence of external load disturbances and unknown parameters and does not have a discrete output. The main drawback of the second-order SMC is complicated mathematical calculations. Likewise, the implementation of this technique will be troublesome if the state variables increase [18]. The integral-SMC–based IM has been improved in ref. [19], by decoupling terms and boundary layer. Although the proposed controller guarantees fast dynamic response, it is sensitive to parameter variations. Super-twisting is a newly developed concept of SMC, which is demonstrated to be effective for electromechanical systems [20]. According to recent advancements in this field, this study presents a super-twisting SMC for controlling torque and realizing loss minimisation strategy, without utilising an internal current loop controller. The proposed controller not only eliminates the chattering effect which occurs in most SMC approaches but also only requires a sliding surface. These are known as main benefits of the super-twisting SMC.

Later in this study, a detailed description of the proposed control system is described. In this regard, the power loss expression is derived in section II and a criterion is determined for the model-based LMA realisation by using a gradient approach. In section III, super-twisting SMC is developed for IM. Finally, the experimental results and concluding remarks are presented in sections IV and V respectively.

2 | MODEL-BASED LOSS MINIMISATION ALGORITHM

2.1 | IM model including iron loss

Space vector equivalent circuit of IM is illustrated in Figure 1. The standard model of IM is achieved from this figure, in RFO frame, as follows [21]:

$$\vec{V}_s = R_s\vec{I}_s + d\vec{\psi}_s/dt + j\omega\vec{\psi}_s \tag{1}$$

$$\vec{V}_r = R_r\vec{I}_r + d\vec{\psi}_r/dt + j(\omega - \omega_r)\,\vec{\psi}_r \tag{2}$$

$$\vec{\psi}_s = L_{ls}\vec{I}_s + L_m\vec{I}_m \tag{3}$$

$$\vec{\psi}_r = L_{lr}\vec{I}_r + L_m\vec{I}_m \tag{4}$$

$$R_i\vec{I}_i = L_m d\vec{I}_m/dt + j\omega L_m\vec{I}_m \tag{5}$$

From Figure 1, the electromagnetic torque is proportional to the rotor flux and torque-producing current (rotor current) and can be derived as follows:

$$T_e = \left(\frac{3}{2}\right).\left(\frac{p}{2}\right).\left(\psi_{rq}i_{rd} - \psi_{rd}i_{rq}\right) \tag{6}$$

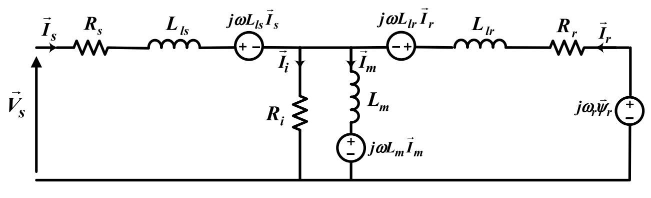

FIGURE 1 Space vector equivalent circuit of induction motor (IM) including iron loss (RFO frame)

The rotor flux orientation is determined by aligning the d-axis of synchronous reference frame with the rotor flux vector $\vec{\psi}_r$. Considering the resultant d- and q-axis rotor flux components, (6) is written as follows:

$$T_e = K_T.\left|\vec{\psi}_r\right|.i_{rq} \tag{7}$$

where $K_T = -3p/4$.

By assuming the steady-state condition, the rotor current components, i_{rd} and i_{rq}, are written as (8) with respect to the stator currents, i_{sd} and i_{sq}:

$$\begin{bmatrix} i_{rd} \\ i_{rq} \end{bmatrix} = \begin{bmatrix} \Delta_1 & -\Delta_2 - \frac{R_r}{\omega_{sl}\ L_m} \\ \Delta_2 & \Delta_1 + \frac{\Delta_2}{\omega_{sl}\ \tau} \end{bmatrix}^{-1} \begin{bmatrix} i_{sd} \\ i_{sq} \end{bmatrix} \tag{8}$$

where $\Delta_1 = -\left(1 + \frac{L_{lr}}{L_m}\right)$ and $\Delta_2 = -\frac{\omega L_{lr}}{R_c}$.

The cross-coupling between d- and q-axis stator currents and rotor currents is avoided by selecting rotor currents as state variables which are responsible for production of electromagnetic torque.

2.2 | Power losses of IM

According to Figure 1, expressions for copper loss and iron loss of IM can be derived as (9)-(11), respectively:

$$P_{cu,s} = R_s\left(i_{sd}^2 + i_{sq}^2\right) \tag{9}$$

$$P_{cu,r} = R_r i_{rq}^2 = R_r\left(\frac{R_c}{R_c + R_r} i_{sq} - \frac{\omega_r L_m}{R_c + R_r} i_{sd}\right)^2 \tag{10}$$

$$P_{iron} = R_i i_{iq}^2 = R_r\left(i_{sq} - i_{rq}\right)^2 \tag{11}$$

Substituting $i_{rq} = \left(\frac{R_c}{R_c + R_r}\right) i_{sq} - \left(\frac{\omega_r L_m}{R_c + R_r}\right) i_{sd}$ into (11), gives (12):

$$P_{iron} = R_r\left(\frac{R_r}{R_c + R_r} i_{sq} + \frac{\omega_r L_m}{R_c + R_r} i_{sd}\right)^2 \tag{12}$$

Thus, total power losses are written as follows:

$$P_{Loss} = \underbrace{\left(R_s + \frac{\omega_r^2 L_m^2}{R_c + R_r}\right)}_{R_d} i_{sd}^2 + \underbrace{\left(R_s + \frac{R_c R_r}{R_c + R_r}\right)}_{R_q} i_{sq}^2 \tag{13}$$

According to (8), expression of power losses is stated in terms of torque-producing currents, as follows:

$$\begin{aligned} P_{Loss} = {} & R_d\left(\Delta_1.i_{rd} - \left(\Delta_2 + \frac{R_r}{\omega_{sl}\cdot L_m}\right).i_{rq}\right)^2 \\ & + Rq\left(\Delta_2.i_{rd} + \left(\Delta_1 + \frac{\Delta_2}{\omega_{sl}\cdot\tau}\right).i_{rq}\right)^2 \end{aligned} \tag{14}$$

2.3 | Affine model of IM

In this section, to get control inputs for the inverter, the super-twisting SMC is applied to the IM drive system. In this regard, $x_1 = i_{rd}$, $x_2 = i_{rq}$, $x_3 = \psi_{rd}$, $x_4 = \psi_{rq}$ and $x_5 = \omega_r$ are defined as state variables, and $V_{sd}^* = u_1$, $V_{sq}^* = u_2$ as inputs. Hence, the state variable model is stated by:

$$\dot{X} = f(X) + g(X).U \tag{15}$$

where

$$X = \left[i_{rd}\ i_{rq}\ \psi_{rd}\ \psi_{rq}\ \omega_r\right]^T,$$

$$U = \left[V_{sd}^*\ V_{sq}^*\right]^T,$$

$$f(X) = \begin{bmatrix} \frac{-L_m}{\sigma.L_s.L_r}\left(\frac{L_s.R_r}{L_m}.x_1 - \left(\frac{\tau_r.R_r.L_{ls}}{L_m} + L_{lr}\right).\omega.x_2 + \frac{L_s}{L_m}.x_4.x_5\right) \\ \frac{-L_m}{\sigma.L_s.L_r}\left(\frac{L_s.R_r}{L_m}.x_2 + \left(\frac{\tau_r.R_r.L_{ls}}{L_m} + L_{lr}\right).\omega.x_1 - \frac{L_s}{L_m}.x_3.x_5\right) \\ -R_r.x_1 + (\omega - x_5).x_4 \\ -R_r.x_2 - (\omega - x_5).x_3 \\ \left(\frac{1}{J}\right).\left(\frac{3p}{4}.(x_1.x_4 - x_2.x_3) - T_l - B.x_5\right) \end{bmatrix}$$

and. $g(X)=[g_1\ g_2]=\frac{-L_m}{\sigma.L_s.L_r}.\frac{R_c}{R_c+R_s}\begin{bmatrix}1 & 0\\ 0 & 1\\ 0 & 0\\ 0 & 0\\ 0 & 0\end{bmatrix}$

2.4 | Control objectives

Minimisation of IM electrical power losses is taken as one of the control objectives. Consistent with the Lagrange's theorem [22], the proposed LMA will be realised when the power losses curve and the torque curve are tangent at a point if and only if their gradient vectors are parallel, so that:

$$\| \nabla T_e(x_1,x_2)\| \ \| \nabla P_{Loss}(x_1,x_2)\| \sin\alpha = 0 \tag{16}$$

The magnitude of the cross-product of $\nabla T_e(x_1,x_2)$ and $\nabla P_{Loss}(x_1,x_2)$ and IM torque are chosen as control outputs, and the output vector $Y=[y_1 \quad y_2]^T$ is introduced as (17) to attain the control objectives:

$$\begin{aligned} y_1 &= \| \nabla T_e(x_1,x_2)\| \ \| \nabla P_{Loss}(x_1,x_2)\| \sin\alpha = \det\begin{bmatrix}\frac{\partial T_e}{\partial x_1} & \frac{\partial T_e}{\partial x_2}\\ \frac{\partial P_{Loss}}{\partial x_1} & \frac{\partial P_{Loss}}{\partial x_2}\end{bmatrix}\\ &= \left((R_d\Delta_1).\left(\Delta_2+\frac{R_r}{\omega_{sl}\,L_m}\right)-(R_q\Delta_2).\left(\Delta_1+\frac{\Delta_2}{\omega_{sl}\,\tau}\right)\right)x_2\\ &\quad -\left(R_d\Delta_1^2+R_q\Delta_2^2\right)x_1\\ y_2 &= T_e = K_T.\left|\vec{\psi}_r\right|.x_2 \end{aligned} \tag{17}$$

If y_1 keeps at zero, the proposed LMA will be realised obviously. Through some calculations on y_1, we have:

$$i_{rd} = i_{rq}\,\xi \tag{18}$$

where $\xi=\left((R_d\Delta_1).\left(\Delta_2+\frac{R_r}{\omega_{sl}\,L_m}\right)-(R_q\Delta_2).\left(\Delta_1+\frac{\Delta_2}{\omega_{sl}\tau}\right)\right)/\left(R_d\Delta_1^2+R_q\Delta_2^2\right)$.

3 | SUPER-TWISTING SLIDING MODE CONTROLLER FOR IM

The aim of the proposed nonlinear controller is to attain fast transient response and minimisation of the steady-state error. To get these purposes, errors of y_1 and y_2 are selected as sliding surfaces:

$$S=[S_1 \quad S_2]^T \tag{19}$$

where $S_1=y_{1,ref}-y_1$ and $S_2=y_{2,ref}-y_2$. If the states of the system reach and remain on the sliding surface, $S=dS/dt=0$

A Lyapunov function candidate is offered in order to achieve conditions on control law that moves the states of the system to the sliding surface:

$$V=\frac{1}{2}S^TS>0 \tag{20}$$

This is a positive definite function and its time derivative is determined as follows:

$$\dot{V}=\frac{1}{2}\left(S^T\frac{dS}{dt}+S\frac{dS^T}{dt}\right)=S^T\frac{dS}{dt} \tag{21}$$

Considering (19), time derivatives of S_1 and S_2 are obtained as follows:

$$\dot{S}=\frac{d}{dt}\begin{bmatrix}S_1\\ S_2\end{bmatrix}=-\frac{d}{dt}\begin{bmatrix}y_1\\ y_2\end{bmatrix} \tag{22}$$

According to (15), (17), and (22), we have:

$$\dot{S}=-\begin{bmatrix}\dot{x}_1-\xi.\,\dot{x}_2\\ K_T.\left|\vec{\psi}_r\right|.\dot{x}_2\end{bmatrix} \tag{23}$$

Using the affine model, (23) is rewritten as (24):

$$\dot{S}=-\begin{bmatrix}\frac{-L_m}{\sigma.L_s.L_r}\left(\frac{L_s.R_r}{L_m}.x_1-\left(\frac{\tau_r.R_r.L_{ls}}{L_m}+L_{lr}\right).\omega.x_2+\frac{L_s}{L_m}.x_4.x_5\right)-\xi.\,\frac{-L_m}{\sigma.L_s.L_r}\left(\frac{L_s.R_r}{L_m}.x_2+\left(\frac{\tau_r.R_r.L_{ls}}{L_m}+L_{lr}\right).\omega.x_1-\frac{L_s}{L_m}.x_3.x_5\right)\\ K_T.\left|\vec{\psi}_r\right|.\frac{-L_m}{\sigma.L_s.L_r}\left(\frac{L_s.R_r}{L_m}.x_2+\left(\frac{\tau_r.R_r.L_{ls}}{L_m}+L_{lr}\right).\omega.x_1-\frac{L_s}{L_m}.x_3.x_5\right)\end{bmatrix} \tag{24}$$

The time derivative of $\dot{S}$ can be also stated as [23]:

$$\dot{S} = A + B.U_{1,2} \tag{25}$$

where

$$A = \begin{bmatrix} \frac{L_m}{\sigma.L_s.L_r}\left(\frac{L_s.R_r}{L_m}.x_1 - \left(\frac{\tau_r.R_r.L_{ls}}{L_m} + L_{lr}\right).\omega.x_2 + \frac{L_s}{L_m}.x_4.x_5\right) \\ -\xi.\frac{L_m}{\sigma.L_s.L_r}\left(\frac{L_s.R_r}{L_m}.x_2 + \left(\frac{\tau_r.R_r.L_{ls}}{L_m} + L_{lr}\right).\omega.x_1 - \frac{L_s}{L_m}.x_3.x_5\right) \\ K_T.\left|\vec{\psi}_r\right|.\frac{L_m}{\sigma.L_s.L_r}\left(\frac{L_s.R_r}{L_m}.x_2 + \left(\frac{\tau_r.R_r.L_{ls}}{L_m} + L_{lr}\right).\omega.x_1 - \frac{L_s}{L_m}.x_3.x_5\right) \end{bmatrix},$$

$B = \frac{L_m}{\sigma.L_s.L_r}.\frac{R_i}{R_i + R_s}.\begin{bmatrix} 1 & -\xi \\ 0 & K_T.\left|\vec{\psi}_r\right| \end{bmatrix}$, and

$$U_{1,2} = \begin{bmatrix} u_1 \\ u_2 \end{bmatrix}$$

Now, the control law which produces the stator voltage vector, is designed such that $dW/dt < 0$ for $S \neq 0$:

$$U_{1,2} = -B^{-1}.\,[A + U^*] \tag{26}$$

where

$$U^* = \int F.\mathrm{sgn}(S) + D|S|^{0.5}\mathrm{sgn}(S)$$

$$F = \begin{bmatrix} F_1 & 0 \\ 0 & F_2 \end{bmatrix},\ D = \begin{bmatrix} D_1 & 0 \\ 0 & D_2 \end{bmatrix},\ \mathrm{sgn}(S) = \begin{bmatrix} \mathrm{sgn}(S_1) \\ \mathrm{sgn}(S_2) \end{bmatrix}^T$$

To prove the stability of sliding surfaces, the time derivative of Lyapunov function (V) should be less than zero ($dV/dt < 0$):

$$\dot{V} = -S.\left(\int F.\mathrm{sgn}(S).dt + D|S|^{0.5}\mathrm{sgn}(S)\right) \tag{27}$$

where $S.sgn(S) > 0$. By selection of proper positive gains, $dV/dt < 0$. As the time derivative of V is a negative definite function, the proposed nonlinear controller becomes asymptotically stable.

4 | RESULTS AND DISCUSSION

The block diagram of the proposed IM super-twisting SMC control is shown in Figure 2. The experimental setup shown in Figure 3 consists of: a TMS320F28335 signal processor board designed with Texas Instrument Co., a voltage source inverter with corresponding driver board, a sensor board, and a 2.2 kW IM. Tables 1 and 2 demonstrate the parameters of the IM and direct current (DC) generators.

The control parameters of the proposed super-twisting SMC are given in Table 3. As shown in Figure 4, the iron loss resistance R_i is experimentally calculated by input power measurement of 2.2 kW IM at the no-load condition. Even though R_i changes with both flux level and operating frequency, it is more sensitive to frequency variations [24].

Figure 5 illustrates the loss minimisation of the induction machine drive implementing the proposed model-based

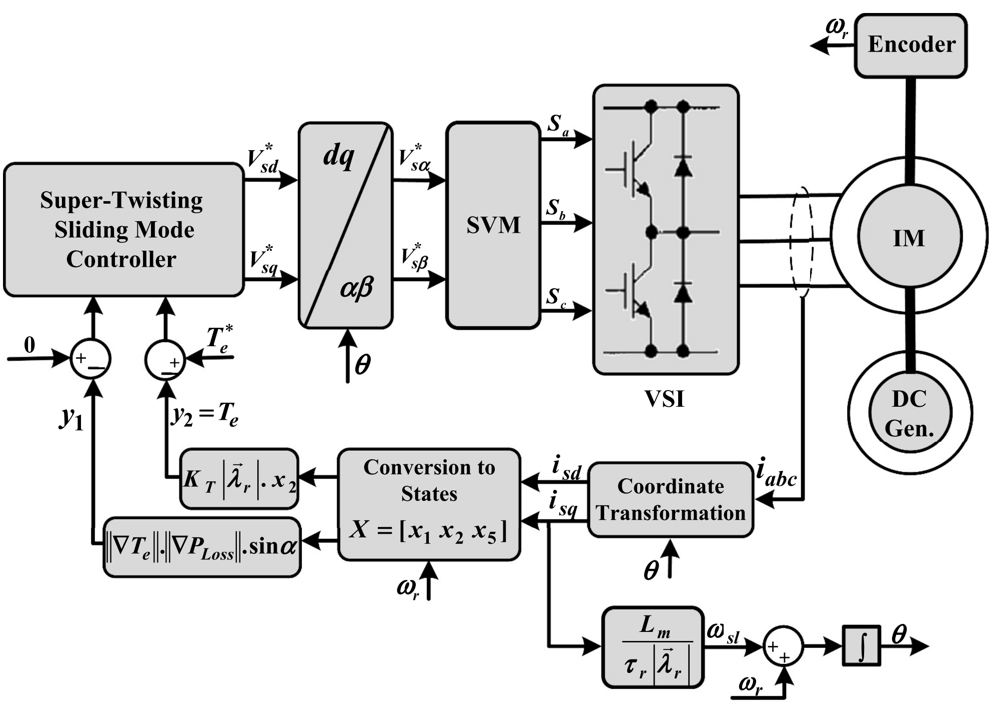

FIGURE 2 Structural block diagram of the proposed loss minimisation algorithms (LMA) based on super-twisting sliding mode controller (SMC)

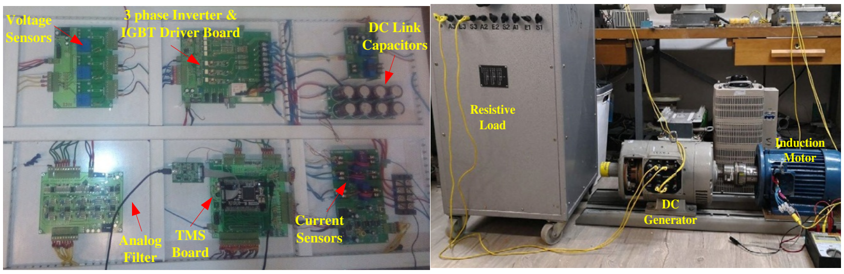

FIGURE 3 Experimental setup

TABLE 1 The 2.2 kW induction motor (IM) parameters

Parameter	Value	Parameter	Value
Rated torque	8	R'_r (Ω)	0.6
Rated voltage (V)	220 (L-L)	$L_{ls} = L'_{lr}$ (H)	0.00365
Rated current (A)	8	L_m (H)	0.2933
R_s (Ω)	0.76	J (kg.m^2)	0.14

TABLE 2 DC generator specifications

Parameter	Value	Parameter	Value
Power (kW)	4.8	Rated current (A)	21
Rated voltage (V)	230	Rotor speed (rpm)	1500

TABLE 3 The super-twisting sliding mode controller (SMC) gains

$F_1 = 23$	$F_2 = 55$	$D_1 = 8$	$D_2 = 14$

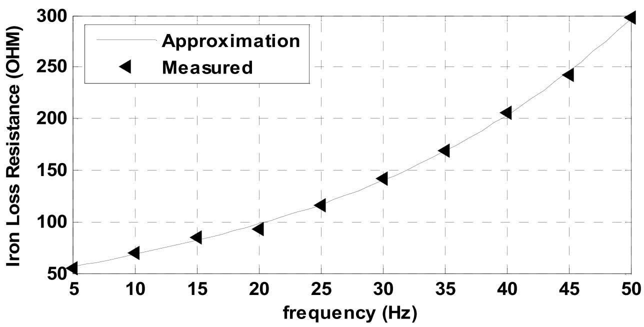

FIGURE 4 Measured iron loss resistance for 2.2 kW induction motor (IM)

strategy. As it is shown, the super-twisting SMC satisfies both control objectives (criterion of LMA realisation (y_1) and torque control (y_2)) and the torque producing current properly follows its reference command. In addition, y_1 oscillates around its reference value ($y_{1,ref} = 0$), which means that the strategy has been realised. The rotor speed linearly decreases and increases. This confirms that the generated torque is fixed at its appropriate value with the aid of the proposed nonlinear controller.

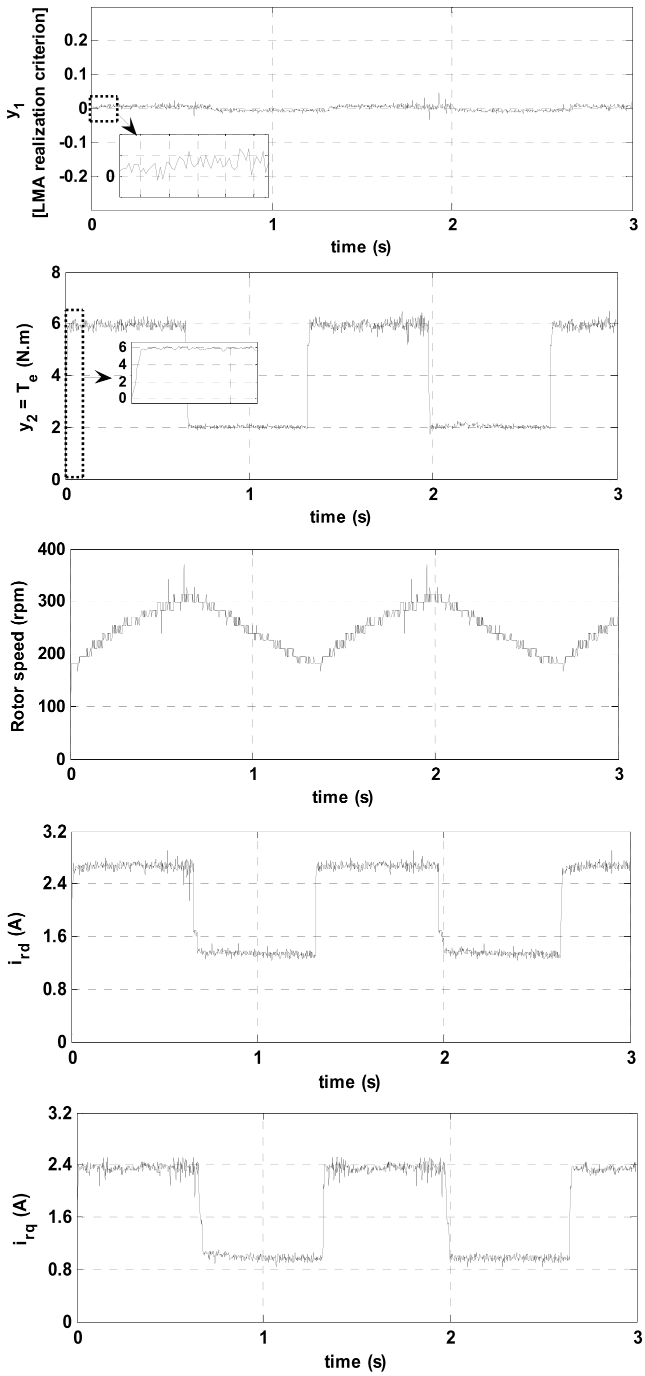

FIGURE 5 Experimental results for efficiency-optimised control strategy

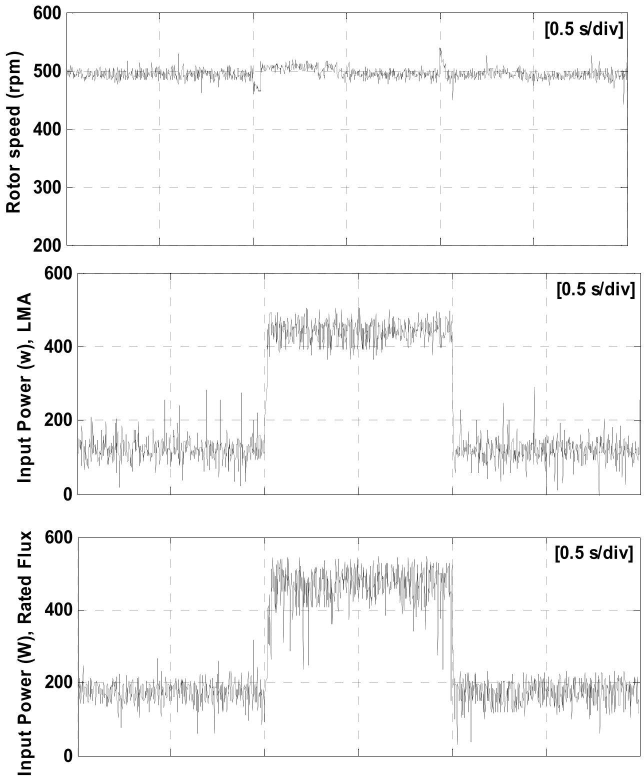

FIGURE 6 Comparison between input power for proposed loss minimisation algorithms (LMA) and input power for rated flux method

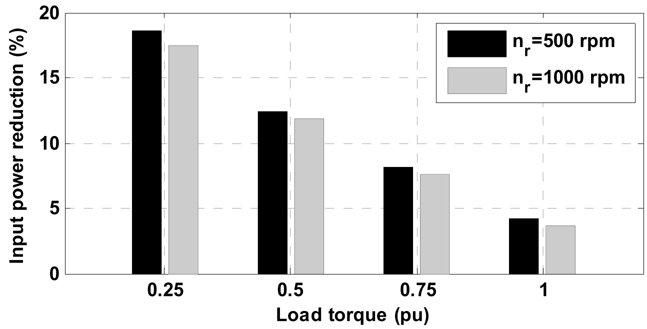

FIGURE 7 Reduction of motor input power with changes in load torque

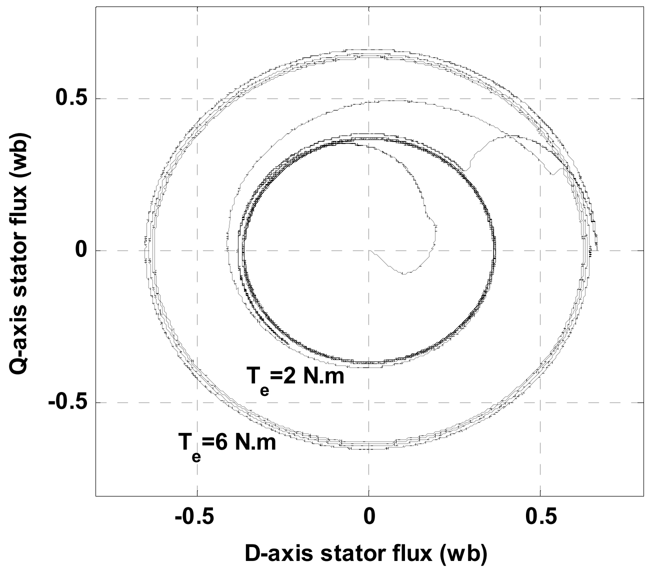

FIGURE 8 The flux linkage trajectory under the proposed loss minimisation algorithms (LMA)

Figure 6 presents the energy optimisation for load variations in constant rotor condition. In this condition, for a 500 rpm reference rotor speed, the load torque alternatively changes from 2 to 6 N.m. As observed, for similar speed and torques, the input power for LMA is lower than the constant flux method. To evaluate the overall performance of the proposed strategy in various torques and rotor speeds, the IM drive is controlled for various load torques from low-load to full load and in two rotor speeds, which are 500 and 1000 rpm (Figure 7). The results confirm that the overall efficiency has been improved, especially in low-load and low-speed conditions. Figure 8 shows how the flux linkage changes with torque under the proposed control strategy. The circle-shaped curve shows that the direct and quadrature components of the stator flux are perpendicular to each other.

5 | CONCLUSION

To accomplish the loss minimisation algorithm, a nonlinear technique was suggested based on super-twisting SMC. The proposed LMA minimises electrical power losses including iron and copper losses by deriving a realisation criterion based on Lagrange's Theorem. The proposed control scheme keeps all benefits of model-based methods such as quick response and high accuracy even during transient condition. In addition, a real-time implementation was accomplished to confirm the effectiveness of the control approach where the high performance of the presented method could be proved. The experimental results showed that the proposed LMA improves IM efficiency, particularly in light load conditions, without deteriorating the dynamic response. In the experiment, the constant flux method and the proposed one were also compared and evaluated. In comparison with the conventional approach, the input power reduction is almost 18.6% and 8.1%, for $T_l = 0.25\,pu$ and $T_l = 0.75\,pu$ respectively.

ACKNOWLEDGEMENTS

The authors wish to express appreciation to Research Deputy of Ferdowsi University of Mashhad for supporting this project by grant no. 50239 (24 August 2019).

CONFLICT OF INTEREST

The authors declare that they have no conflict of interest.

DATA AVAILABILITY STATEMENT

The data that support the findings of this study are available from the corresponding author upon reasonable request.

NOMENCLATURE

$\vec{V}$, $\vec{I}$, $\vec{\psi}$	Voltage, current, and flux vectors
T_e	Electromagnetic torque
P	Power loss
T_l	Load torque
R	Resistance
L	Self-inductances of stator and rotor
L_l	Leakage inductances of stator and rotor
L_m	Coupling inductance between stator and rotor
σ	Leakage factor $\left(1-\left(L_m^2/L_s.L_r\right)\right)$
τ_r	Rotor time constant (L_r/R_r)
τ	Time constant (L_{lr}/R_r)
p	Pole pair
ω_r, ω	Angular speed of rotor and flux
$\omega_{sl} = \omega - \omega_r$	Slip speed
J	Moment of inertia
B	Friction coefficient
X	State variables vector
U	Control inputs
Y	Output vectors
S	Sliding surface
V	Lyapunov's function
α	Angle between gradient vectors
θ	Rotor flux orientation angle
e	Error
F, D	Positive Control gains

SUBSCRIPTS

s, r	Stator and rotor
m	Magnetising
i	Iron loss
d, q	Rotating direct and quadrature axes
cu, $core$	Copper and iron

ORCID

Hamidreza Mosaddegh Hesar https://orcid.org/0000-0002-0297-3135
Mojtaba Ayaz Khoshhava https://orcid.org/0000-0003-4989-3260
Hossein Abootorabi Zarchi https://orcid.org/0000-0002-3512-2302

REFERENCES

1. Yamamoto, S.: Overview of the latest research and development for copper die-cast squirrel-cage rotors. Int. Power Elec. Conf. 1949–1954 (2018)
2. Yousefian, M., Mosaddegh Hesar, H., Abootorabi Zarchi, H.: Optimal design of a single-phase two-value capacitor induction motor with fan load. Iranian Conf. Elec. Eng. (ICEE), 1298–1303 (2018)
3. Uddin, M.N., Nam, S.W.: Development of a nonlinear and model-based online loss minimization control of an IM drive. IEEE Trans. Energy Convers. 23(4), 1015–1024 (2008). https://doi.org/10.1109/tec.2008.2001442
4. Kirschen, D.S., Novotny, D.W., Lipo, T.A.: On line efficiency optimization of a variable frequency induction motor drive. IEEE Trans. Ind. Appl. IA-21(3), 610–616 (1985). https://doi.org/10.1109/tia.1985.349717
5. Borisevich, A., Schullerus, G.: Energy efficient control of an induction machine under torque step changes. IEEE Trans. Energy Convers. 31(4), 1295–1303 (2016). https://doi.org/10.1109/tec.2016.2561307
6. Hu, D., Xu, W., Dian, R., Liu, Y., Zhu, J.: Loss minimization control of linear induction motor drive for linear metros. IEEE Trans. Ind. Electron. 65(9), 6870–6880 (2017). https://doi.org/10.1109/tie.2017.2784343
7. Farhani, F., Regaya, C.B., Zaafouri, A.: Real time PI-Back-Stepping induction machine drive with efficiency optimization. ISA Trans. 70, 348–356 (2017). https://doi.org/10.1016/j.isatra.2017.07.003
8. Sridharan, S., Krein, P.T.: Minimization of system-level losses in VSI-based induction motor drives: offline strategies. IEEE Trans. Ind. Appl. 53(2), 1096–1105 (2017). https://doi.org/10.1109/tia.2016.2631513
9. Yu, J., Pei, W., Zhang, C.: A loss-minimization port-controlled Hamilton scheme of induction motor for electric vehicles. IEEE/ASME Trans. Mech. 20(6), 2645–2653 (2015). https://doi.org/10.1109/tmech.2014.2361030
10. Kumar, N., Chelliah, T.R., Srivastava, S.: Adaptive control schemes for improving dynamic performance of efficiency-optimized induction motor drives. ISA Trans. 57, 301–310 (2015). https://doi.org/10.1016/j.isatra.2015.02.011
11. Kaboli, S., Zolghadri, M.R., Vahdati-Khajeh, E.: A fast flux search controller for DTC-based induction motor drives. IEEE Trans. Ind. Electron. 54(5), 2407–2416 (2007). https://doi.org/10.1109/tie.2007.900341
12. Hajian, M., Arab Markadeh, G.R., Soltani, J.: Energy optimized sliding-mode control of sensorless induction motor drives. Energy Convers. Manag. 50(9), 2296–2306 (2009). https://doi.org/10.1016/j.enconman.2009.05.006
13. Shreelakshmi, M.P., Agarwal, V.: Trajectory optimization for loss minimization in induction motor fed elevator systems. IEEE Trans. Power Electron. 33(6), 5160–5170 (2018). https://doi.org/10.1109/tpel.2017.2735905
14. Chakraborty, C., Hori, Y.: Fast efficiency optimization techniques for the indirect vector-controlled induction motor drives. IEEE Trans. Ind. Appl. 39(4), 1070–1076 (2003). https://doi.org/10.1109/tia.2003.814550
15. Vukosavic, S.N., Levi, E.: Robust DSP-based efficiency optimization of a variable speed induction motor drive. IEEE Trans. Ind. Electron. 50(3), 560–570 (2003). https://doi.org/10.1109/tie.2003.812468
16. Lascu, C., Boldea, I., Blaabjerg, F.: Variable-structure direct torque control-A class of fast and robust controllers for induction machine drives. IEEE Trans. Ind. Electron. 51(4), 785–792 (2004). https://doi.org/10.1109/tie.2004.831724
17. Barambones, O., Garrido, A., Maseda, F.: Integral sliding-mode controller for induction motor based on field-oriented control theory. IET Control Theory & Appl. 1(3), 786–794 (2007). https://doi.org/10.1049/iet-cta:20060239
18. Bartolini, G., Fridman, L., Pisano, A., Usai, E.: Modern Sliding Mode Control Theory, New Perspectives and Applications. Springer: New York (2008)
19. Comanescu, M., Xu, L., Batzel, T.D.: Decoupled current control of sensorless induction-motor drives by integral sliding mode. IEEE Trans. Ind. Electron. 55(11), 3836–3845 (2008). https://doi.org/10.1109/tie.2008.2003201
20. Evangelista, C., Puleston, P., Valenciaga, F., Fridman, L.: Lyapunov-designed super twisting sliding mode control for wind energy conversion

optimization. IEEE Trans. Ind. Electron. 60(2), 538–545 (2013). https://doi.org/10.1109/tie.2012.2188256
21. Levi, E.: Impact of iron loss on behavior of vector controlled induction machines. IEEE Trans. Ind. Appl. 31(6), 1287–1296 (1995). https://doi.org/10.1109/28.475699
22. Lee, H., Kang, S.J., Sul, S.K.: Efficiency-optimized direct torque control of synchronous reluctance motor using feedback linearization. IEEE Trans. Ind. Electron. 46(1), 192–198 (1999). https://doi.org/10.1109/41.744411
23. Sadeghi, R., Madani, S.M., Ataei, M., Agha Kashkooli, M.R., Ademi, S.: Super-twisting sliding mode direct power control of brushless doubly fed induction generator. IEEE Trans. Ind. Electron. 65(11), 9147–9156 (2018). https://doi.org/10.1109/tie.2018.2818672
24. Matsuse, K., Yoshizumi, T., Katsuta, S., Taniguchi, S.: High-response flux control of direct-field-oriented induction motor with high efficiency taking core loss into account. IEEE Trans. Ind. Appl. 35(1), 62–69. Jan/Feb. 1999. https://doi.org/10.1109/28.740846

How to cite this article: Hesar, H.M., Khoshhava, M.A., Zarchi, H.A.: Model-based online efficiency control of induction motor drives based on nonlinear technique. IET Electr. Power Appl. 1–9 (2022). https://doi.org/10.1049/elp2.12222